International Journal of Power Electronics and Drive System (IJPEDS)
Vol. 8, No. 2, June 2017, pp. 612~622
ISSN: 2088-8694, DOI: 10.11591/ijpeds.v8i2.pp612-622

Speed and Position Estimator of Dual-PMSM for Independent Control Drives using Five-Leg Inverter

Jurifa Mat Lazi[1], Zulkifilie Ibrahim[2], MD Hairul Talib[3], Auzani Jidin[4], Tole Sutikno[5]
[1,2,3,4]Department of Power Electronics and Drives, Faculty of Electrical Engineering, Universiti Teknikal Malaysia Melaka (UTeM), Hang Tuah Jaya, 76100 Durian Tunggal, Melaka, Malaysia
[5]Department of Electrical Engineering, Faculty of Industrial Technology, Universitas Ahmad Dahlan, Yogyakarta, Indonesia

Article Info

Article history:

Received Jan 28, 2017
Revised Mar 28, 2017
Accepted Apr 9, 2017

Keyword:

Dual-PMSM
Five-Leg inverter
Sensorless
Speed estimator
SVPWM

ABSTRACT

Nowadays, A lot of industry requires Multi Motor System (MMS) applications such as propulsion and traction power, HEV, conveyer and air-conditioner. The Conventional arrangement for MMS usually done by cascading the motors drives which each drives has individual inverter. Part of MMS, Dual-Motor drives fed by a single inverter is being paid attention by the researchers. Dual-motor drives using a single three-leg inverter has its limitation in the case of different operating conditions and independent speed control requirement. Therefore, dual-Motor drives using a single Five-leg Inverter (FLI) was proposed for independent control for both motors. In PMSM drives, the information of the feedback speed and rotor angular position is compulsory for variable speed drives. Conventional solution is by using speed sensor which will increase size, cost, extra hardwire and feedback devices, especially for the case of dual-PMSM drives. The best solution to overcome this problem is by eliminating the usage of speed and position sensors for Dual-motor drives. This paper presents a new sensorless strategy using speed and position estimator for Independent Dual- Permanent Magnet Synchronous Machine (PMSM) drives which utilize Five-Leg Inverter (FLI). The proposed strategy is simulated using MATLAB/Simulink to evaluate the overall motor drive performance. Meanwhile the experimental set-up is connected to dSPACE 1103 Board. The experimental results demonstrate that the proposed estimator is successfully managed to control the Dual-PMSM drives for variation of speed and for different direction applications.

Corresponding Author:

Jurifa binti Mat Lazi,
Department of Power Electronics and Drives, Faculty of Electrical Engineering,
Universiti Teknikal Malaysia Melaka,
Hang Tuah Jaya, 76100, Durian Tunggal, Melaka, Malaysia.
Email: jurifa@utem.edu.my

1. INTRODUCTION

Dual-Motor drives using Five-Leg Inverter (FLI) is designed to provide an individually control for the dual-motor drives which can be controlled independently for different types of operating condition. FLI topology consists of ten switches, where one of the legs is commonly shared by the Dual PMSMs as illustrated in Figure 2. It also proven that dual-motor can be operated independently at different operating condition by using FLI topology [1]-[5]. Independent control for dual-motor fed by FLI was introduced by Francois and Bouscayrol in 1999 [6] specifically for Induction Machine (IM). The idea of FLI was proven can be used to control for different rotations speeds on both motors. In addition, they try to extend the capability of the FLI in AC-AC converter in order to supply a single IM with unitary power factor [7].

However, those researches are only present in simulation results only. Only in 2003, they come out with the experimental prove that FLI topology is able to control dual-motor for different applications [5]. Since then, many researchers are giving attentions to this topology and came out with different strategies [1-12].

Based on the literature, this current study utilizes Space Vector Pulse Width Modulation (SVPWM) method [1], since this is the simplest and easiest method to implement using single processor. Other than that, this technique utilizes standard three-phase modulators to generate modulation signals for all legs of a FLI. The modulation technique that is being used in this current study is depicted in Figure 2.

In the case of conventional Five-Leg Inverter (FLI), a lot of external wires, sensors are needed because it deals with the two sets of current sensors, two sets of encoders or resolvers in order to capture the information of rotor position. The appearance of all the transducers increases the total size and costs of the drives. Because of these problems, this current study proposes the sensorless technique for dual-PMSM drive using FLI in order to reduce the drive space and to lower overall cost by eliminating the mechanical position sensor. Nevertheless, the performance of this sensorless technique are almost similar to the drive that using sensor.

Various techniques in sensorless strategy are discussed by different researchers. Most of the techniques are based on the voltage equations of the PMSM and the information of the terminal quantities, such as line voltage and phase current. By using this information, the rotor angle and speed are estimated directly or indirectly. Basically, estimation of the sensorless techniques can be based on different categories; Back Electromagnetic Force, Excitation Monitoring, Motor Modification, Magnetic Saliency, Observer and Signal injection. Therefore, adaptive model based on voltage and current method is selected as the sensorless technique for this current study.

2. DESIGN OF SENSORLESS SPEED CONTROL FOR DUAL PMSM DRIVES

This current study introduces a sensorless technique using adaptive control based on differential of d-q currents and voltages to estimate the speed of motors “1” (m1) and motor “2” (m2). The basic diagram for overall block diagram is depicted in Figure 1. This figure shows the overall block diagram of the proposed method which consist of two sets of PMSM drive, single FLI, speed controller and the speed and position estimator for each motor. The output of three-phase voltages and currents for both motors are measured. These currents and voltages are being used in the speed estimator. The estimator will produce the estimated value of motor’s speed. The estimated rotor position is calculated by integrating the value of the motor speed.

.

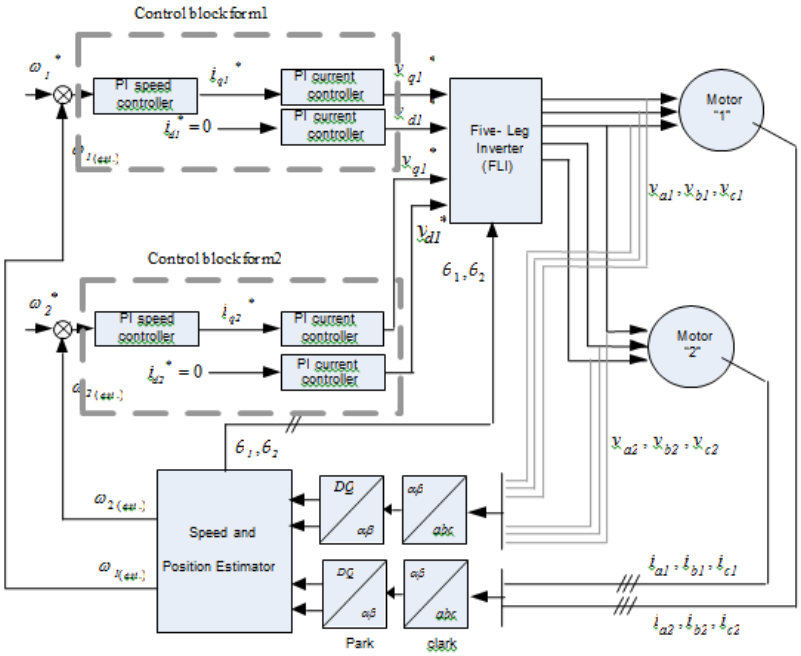

Figure 1. Block diagram of the proposed method

2.1. Five-Leg Inverter for Dual-PMSM

Five-Leg Inverter (FLI) consists of ten switches, which one of the leg is commonly shared by Dual PMSMs as depicted in Figure 2. Two PMSMs share the inverter leg *3* that connected to phase c_1 and c_2. While legs *1* and *2* are connected to phases a_1 and b_1 respectively of the m1. Inverter legs *4* and *5* are connected to phases a_2 and b_2, respectively of the m2. Voltage of DC link (V_{dc}) is considered as rated voltage for operating range of one machine can be achieved [3]. FLI topology offers saving of two switches when compared to the standard dual-three-phase voltage source inverter configuration. Thus, it can reduce the complexity of the inverter structure and also possibility to control dual three-phase motors using only single processor.

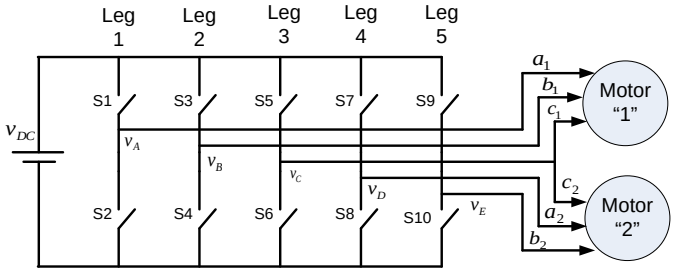

Figure 2. Dual-PMSM fed by Five-Leg Inverter (FLI)

2.2. Modulation Technique

Different modulation techniques are applied throughout the literature [1-3, 5, 9, 10]. This current study is using Space Vector Pulse Width Modulation (SVPWM) method that is being used in [1], since this is the simplest method and very easy to implement using single processor. Other than that, this method utilizes standard three-phase modulators to generate modulation signals for all legs of a FLI.

Figure 3 shows the configuration of dual SVPWMs for FLI, Dual Motor drives. The output for SVPWM is arranged in that particular way in order to reduce the number of modulating signal from six to five. The outputs of five modulating signals for inverter legs are explained:

$$\begin{aligned} \delta_A &= \delta_{a1} + \delta_{c2} \\ \delta_B &= \delta_{b1} + \delta_{c2} \\ \delta_C &= \delta_{c1} + \delta_{c2} \\ \delta_D &= \delta_{a2} + \delta_{c1} \\ \delta_E &= \delta_{b2} + \delta_{c1} \end{aligned} \tag{1}$$

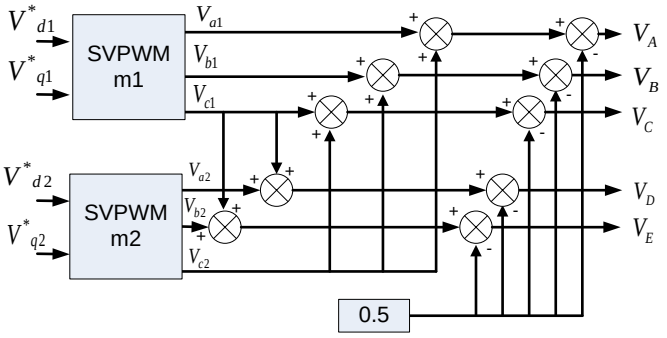

Figure 3. Space Vector Pulse Width Modulation for FLI, Dual-Motor drives

Where subscripts "1" and "2" represent m1 and m2 respectively. From equation (1), the signal of δ_{c2} is added to the modulating signals coming from the m1 PWM modulator. This signal has no effect on the voltages of the m1 since it appears as a zero-sequence component and it gets cancelled in the line-to-line voltages of m1. This sequence is similar to signal $\delta_{c1,}$ which is added to the output of m2 modulator. It does not affect any operation m2. Let say the switching period, t_s is equal to "1". The value of the duty cycles for each space vector modulator is between "0" and "1". When the reference input is equal to zero, the resulting duty cycle is about 0.5. By referring to equation (1), the summation duty cycle between m1 and m2 will be shifted between the ranges 0.5 to 1.5. These new range is not fit for the switching period value. Therefore, 0.5 need to be withdrawn from the equation (1) as shown in Figure 3. Application time for zero space vector "III" is increasing effectively while the application time for zero space vector "000" is decreasing before shifted to "-0.5" without affecting to application time for two active space vectors. This chronology is similar to m2 by referring to equation (1).

Figure 4 shows the space vector modulator operation, which Figure 4(a) and (b) present the reference space vectors with $V_{1,ref} = 0.3V_{dc}\angle 45^0$ for m1 located in sector I, and $V_{2,ref} = 0.2V_{dc}\angle 140^0$ for m2 located in sector II respectively. The dashed boxes represent the time duration and the active space vectors for both m1 and m2 in Figure 4(c) and (d). Meanwhile Figure 4(e) shows the resulted combined SVPWM switching pattern for FLI. It is proven that total zero vector time durations for m1 and m2 are still similar as for individually SVPWM.

Thus, the identical space vectors of each motor are completed each other and the space vector modulator is able to fulfil the requirements of the both motors. It also can be seen that, at the remaining next part which space vectors reference of each motor are contradicting, and the requirements of one motor are met, the second machine will receive zero space vector (000 or III). This shows that all of 32 switching states for FLI are utilised and there are no limit to use all the available states. The resultant PWM signal is symmetrical and this makes FLI topology can be implemented using single standard microprocessor.

2.3. Mathematical Model for Dual PMSMs Drives

The mathematical model for m1 and m2 in d-q, synchronous rotating reference frame can be determined by following equations [15]-[16] respectively.

$$v_{d1} = r_{s1} i_{d1} + \frac{d}{dt}\psi_{d1} - \omega_{e1}\psi_{q1} \tag{2}$$

$$v_{q1} = r_{s1} i_{q1} + \frac{d}{dt}\psi_{q1} + \omega_{e1}\psi_{d1} \tag{3}$$

$$v_{d2} = r_{s2} i_{d2} + \frac{d}{dt}\psi_{d2} - \omega_{e2}\psi_{q} \tag{4}$$

$$v_{q2} = r_{s2} i_{q2} + \frac{d}{dt}\psi_{q2} + \omega_{e2}\psi_{d} \tag{5}$$

Where;

v_d , v_q : *d-q* axis voltage

i_d , i_q : *d-q* axis currents

ω_e : electrical speed of motor

r_s : stator resistance

ψ_d , ψ_q : *d-q* axis flux linkages

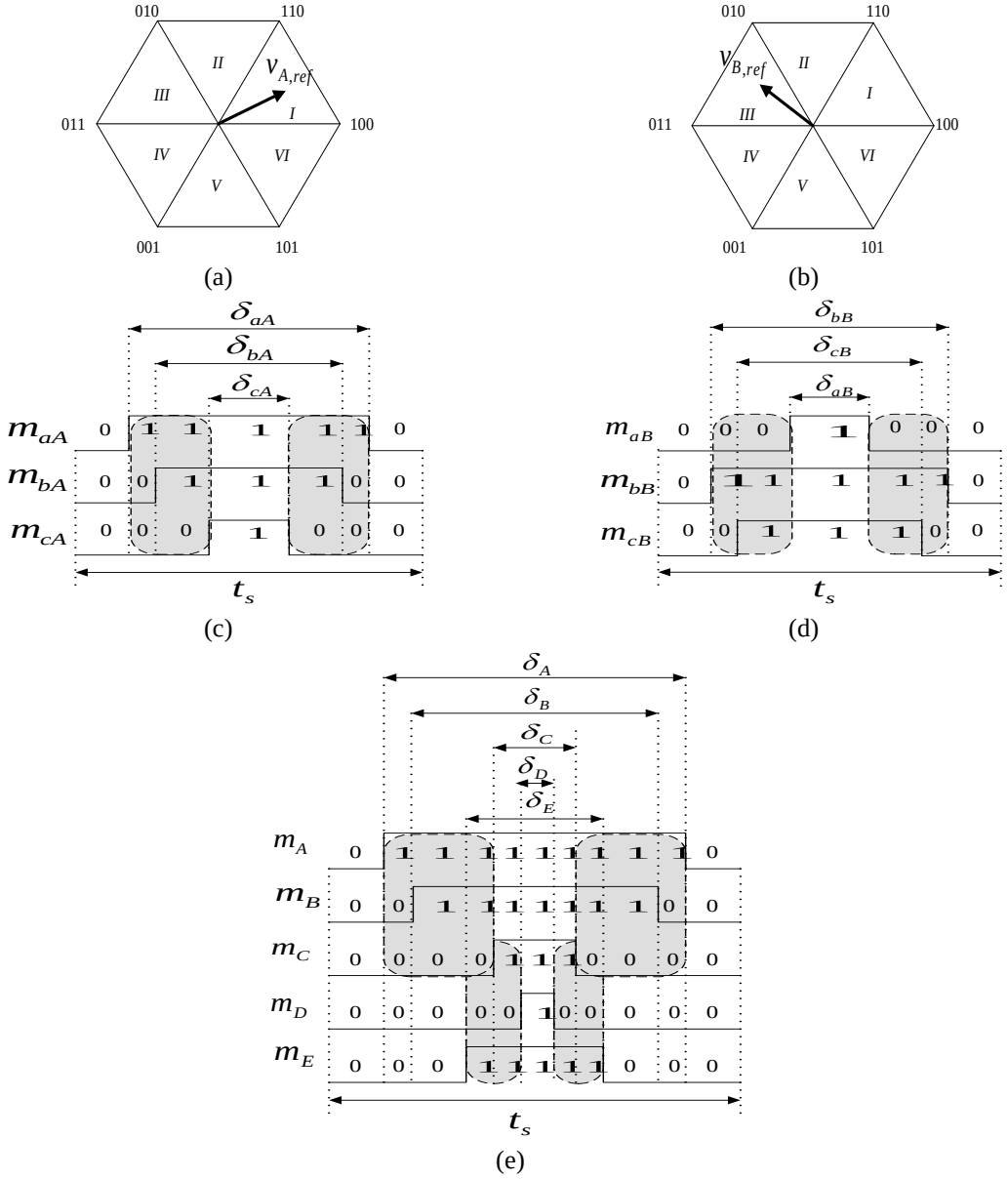

Figure 4. Space Vector PWM (SVPWM) and the switching pattern for the FLI; a)Space Vector reference for *m1*, b) Space Vector reference for *m2*, c) Switching pattern for *m1*, d) Switching pattern for *m2*, e) Switching pattern for the Five-Leg Inverter (FLI)

The flux linkages ψ_d and ψ_q can be expressed in term of stator currents and constant flux linkage ψ_m due to rotor permanent magnet as:

$$\psi_{d1} = L_{d1} i_{d1} + \psi_{m1} \tag{6}$$

$$\psi_{q1} = L_{q1} i_{q1} \tag{7}$$

$$\psi_{d2} = L_{d2} i_{d2} + \psi_{m2} \tag{8}$$

$$\psi_{q2} = L_{q2} i_{q2} \tag{9}$$

Where;

L_d, L_q : *d-q* axis inductances

By substituting equation (6) to (9) into equations (2) to(5), the new equations for stator voltages are formulated;

$$v_{d1} = r_{s1} i_{d1} + L_{d1} \frac{d}{dt} i_{d1} - \omega_{e1} L_{q1} i_{q1} \tag{10}$$

$$v_{q1} = r_{s1} i_{q1} + L_{q1} \frac{d}{dt} i_{q1} + \omega_{e1} L_{d1} i_{d1} + \omega_e \tag{11}$$

$$v_{d2} = r_{s2} i_{d2} + L_{d2} \frac{d}{dt} i_{d2} - \omega_{e2} L_{q2} i_{q2} \tag{12}$$

$$v_{q2} = r_{s2} i_{q2} + L_{q2} \frac{d}{dt} i_{q2} + \omega_{e2} L_{d2} i_{d2} + \tag{13}$$

The electromagnetic torque is

$$T_{em1} - T_{L1} = J \frac{d\omega_{r1}}{dt} \tag{14}$$

With $T_{em1} = \frac{3}{2} p \times real\{i_1 \psi_{r1}\}$ (15)

$$T_{em2} - T_{L2} = J \frac{d\omega_{r2}}{dt} \tag{16}$$

with $T_{em2} = \frac{3}{2} p \times real\{i_2 \psi_{r2}\}$ (17)

And the instantaneous angular position is;

$$\theta_1 = \int \omega_{r1} dt \tag{18}$$

$$\theta_2 = \int \omega_{r2} dt \tag{19}$$

Since the flux produced by permanent magnets has been assumed to be constant, the electromagnetic torque can be varied by changing the magnitude and the phase of the stator current. Thus, a constant torque is obtained if the quadrature axis component of the stator current space vector is kept constant and the max torque per Ampere of stator current is obtained if the torque angle is 90^0. This corresponds to the application of imaginary axis only for the above stator current equation.

2.4. Design of Speed and Position Estimator

Figure 5 represents the configuration of speed and position estimation scheme. It consists of three-phase to two-phase conversion, adjustable model and adaptation mechanism. The goals in the design are reducing the noise impact to control and influence the system transient response as small as possible. Firstly, the three-phase voltage and current are converted to d-q model. Then, the d-q currents and voltages are being used in Adjustable Model and Adaptation Mechanism respectively. From Equation (10) to (13) , the phase conversion and adjustable model equations can be formulated as (20) to (23):

$$\frac{d}{dt}\hat{i}_{d1(k+1)} = \frac{(v_{d1}^{*}(k) - r_{s1}\hat{i}_{d1(k)} + \hat{\omega}_{e1(k)}L_{q1}\hat{i}_{q1(k)})}{L_{d1}} \tag{20}$$

$$\frac{d}{dt}\hat{i}_{q1(k+1)} = \frac{(v_{q1}^{*}(k) - r_{s1}\hat{i}_{q1(k)} - \hat{\omega}_{e1}L_{d1}\hat{i}_{d1(k)} - \hat{\omega}_{e1}\psi_{m1})}{L_{q1}} \tag{21}$$

$$\frac{d}{dt}\hat{i}_{d2(k+1)} = \frac{(v_{d2}^{*}(k) - r_{s2}\hat{i}_{d2(k)} + \hat{\omega}_{e2(k)}L_{q2}\hat{i}_{q2(k)})}{L_{d2}} \tag{22}$$

$$\frac{d}{dt}\hat{i}_{q2(k+1)} = \frac{(v_{q2}^{*}(k) - r_{s2}\hat{i}_{q2(k)} - \hat{\omega}_{e2}L_{d2}\hat{i}_{d2(k)} - \hat{\omega}_{e2}\psi_{m2})}{L_{q2}} \tag{23}$$

Where "^" is referring to estimated value

The output of conversion three-phase model is estimated *d-q* current which is compared with actual *d-q* axis currents. These currents are used to calculate the estimated speed through adaptation mechanism. The adaptation mechanism is designed in order to improve the stability and behavior of the adaptive system. It is calculated using Popov's hyper-stability theory to derive the estimated speed as in equation (24).

$$\hat{\omega}_{est} = \left(k_p + \frac{k_i}{s}\right)\varepsilon \tag{24}$$

$$\varepsilon = \left(i_d \times \hat{i}_{q\,est}\right) - \left(i_q \times \hat{i}_{d\,est}\right) - \frac{\psi_m}{L}\left(i_q - \hat{i}_{q\,e}\right. \tag{25}$$

An estimation error defined by equation ((25) is derived when the speed used in the current model is not identical to actual model without any influence of parameter variation. A tuning signal for adjustable model is generated from the regulation of this error through a PI controller. The process continues till the error between two outputs tends to zero.

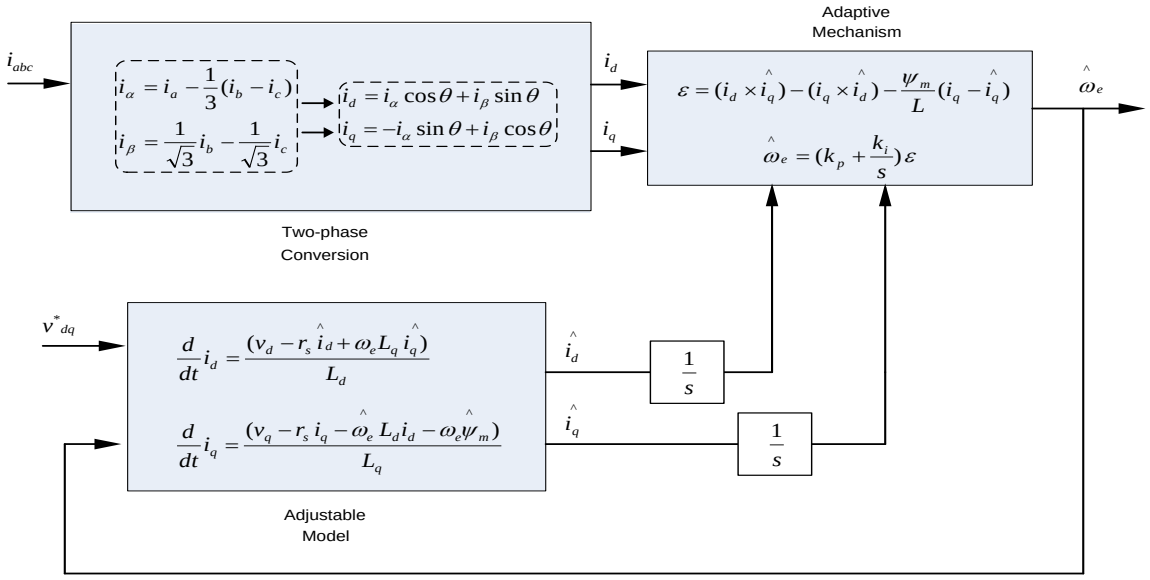

Figure 5. Configuration of speed and position estimator for a single PMSM and applicable for m1 and m2 respectively.

2.5. Hardware Implementation

The hardware implementation consists of PC, VSI, PMSM and Hall-effect current sensors. The control board for drive system is dSPACE DS1103. The dSPACE has been supplemented by a set of on-board peripherals used in digital control systems such as A/D and D/A converters. The DS1103 is equipped with a TMS320F240 that acts as slave processor for advanced I/O purposes. The power circuit of the drives is composed of IGBT based five-phase VSI and gate driver circuits. The specification of VSI is given in Appendix. The VSI is advised to operate at 50 kHz maximum switching frequency and can supply up to 46A. The DC link voltage of 300V for the VSI is achieved through DC power supply module. In this VSI, the dead-time of 3.0μs is applied to each switching transition to prevent a shoot-through fault or short-circuit fault. The model of PMSMs is BSM90N-1150 from BALDOR. The motor's parameters are presented in Table 1. The Experimental set-up for the overall system is depicted in Figure 6.

The model and analysis of the sensorless speed PMSM drives is done using MATLAB/Simulink environment. The model is downloaded to the input/output connection via Real Time (RTI) library. The implementation of the model is carried out on RTI hardware through dSPACE expansion box. After verification in a real environment, the outputs are monitored and tuned through Graphical User Interface (GUI) in dSPACE Control Desk. Then the output of the system such as speed, rotor position and three-phase currents are measured and used as system feedback through dSPACE's Analog to Digital (ADC) ports.

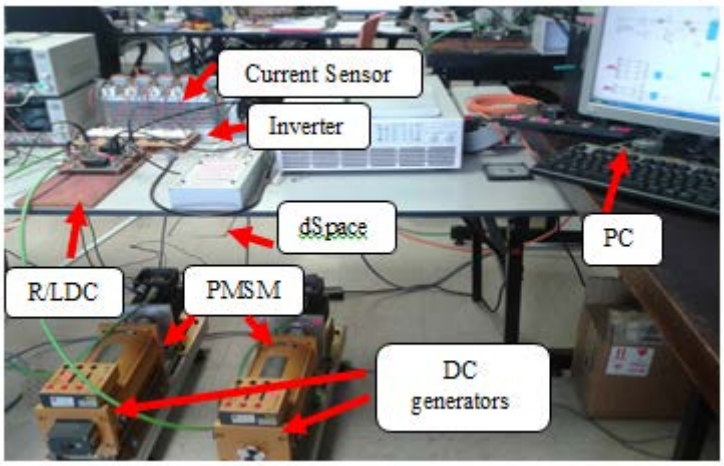

Figure 6. Experimental set-up for sensorless speed control for PMSM drives

3. RESULTS AND ANALYSIS

Figure 7 and Figure 8 represent the detailed behavior of speed responses for Dual PMSMs. The relevant parameters for m1 and m2 are listed in Table 1. Both motors have same parameters and specifications. Both PMSM motors are tested under following different operating conditions; (a) Forward and Reverse Operation and (b)Load disturbance. The test was conducted as follows; for m1, the step speed command is in forward operation (240 RPM) was applied at t=3.9s. The speed command was changed from forward to reverse operation (-240 RPM) at t=13.3s. Then, the command was changed again to forward operation (240 RPM) at t=24s. Meanwhile, for m2, the step speed command is in reverse operation (-240 RPM) was applied at t=7.9s. The speed command was changed from reverse to forward operation (240 RPM) at t=17.3s. Then, the command was changed again to reverse operation (-240 RPM) at t=29.2s.

3.1. Forward and Reverse Operation

Figure 7 presents the forward and reverse operation of Dual-PMSM Drives using Sensorless Control Technique. From the observation, the sensorless drives system managed to run forward and reverse operation at low speed. Basically, in simulatian, unloaded condition will create almost zero current flow; unfortunately, there were small three-phase current induced in current responses for m1 and m2 due to inertia and some inaccuracies in experimental set-up such. Similar to the quadrature iq, also affected by the increase of three phase current which depicted in Figure 7(d) and (e).

For load disturbance condition, the DC motors needs to be attached to both m1 and m2. But only one motor is connected to load bank. The load disturbance was investigated by applying external load

disturbance at -600RPM for m2. The load disturbance was applied at t = 27.5s. The PMSM drives experienced small undershoot during the load rejection period as shown in Figure 8.

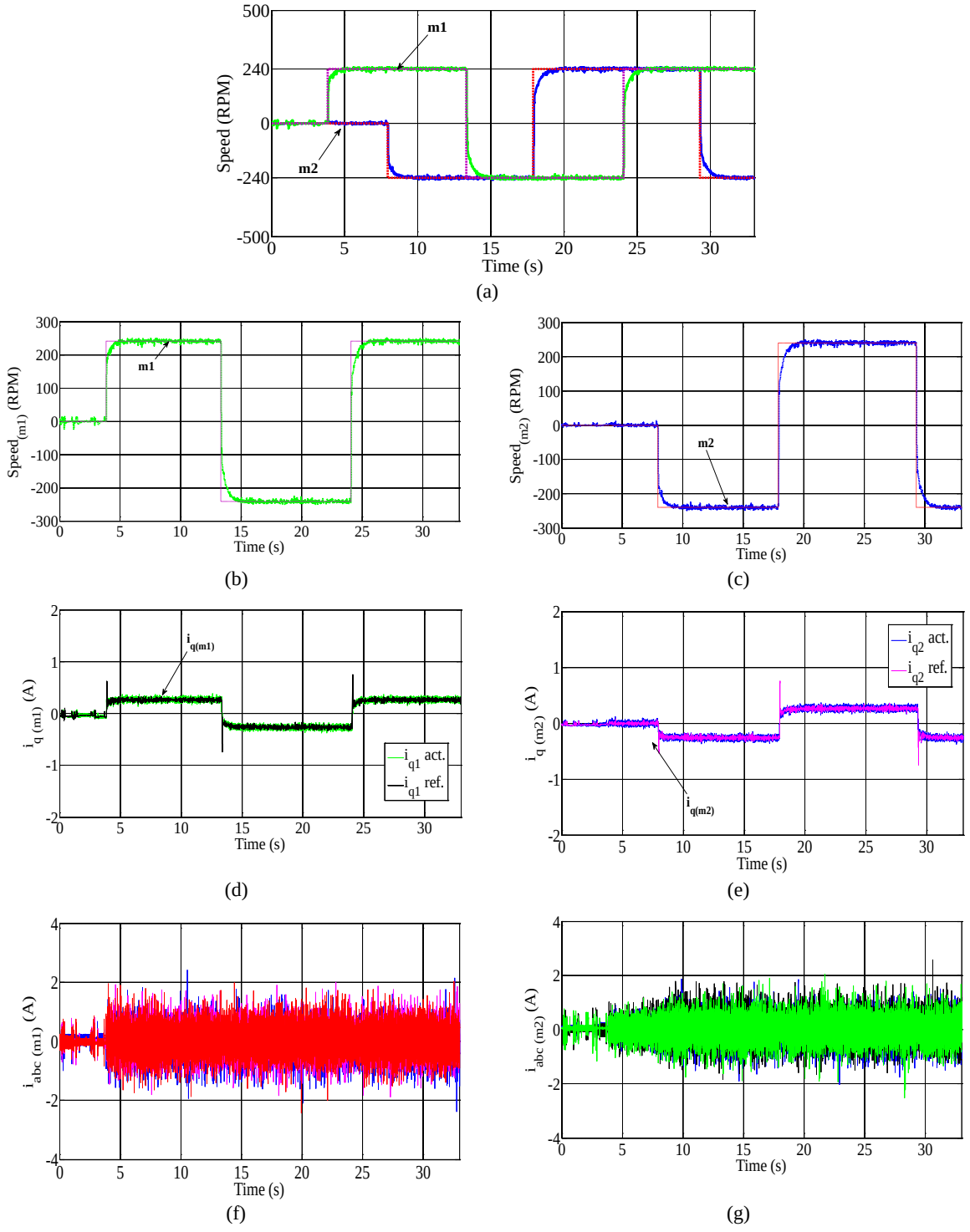

Figure 7. (a) - Speed responses for m1 and m2 during forward and reverse operation, (b) – Speed response for m1, (c) – Speed response for m2, (d) – quadrature current i_q for m1, (e) – quadrature current i_q for m2, (f) – three-phase current i_{abc} for m1, (g) – three-phase current i_{abc} for m2.

3.2. Load Disturbance

The reliability of the Dual-PMSM Drives using sensorless control technique was examined through Figure 8. Due to hardware limitation, only one motor which was m1 experience the load rejection at t=27.55s, meanwhile m2 was remain constant at 600 RPM without any load disturbance. As the torque and speed of the motor change, there must be changes too in direct and qudrature currents. This is due to the production of the direct and qudrature current are based on the transformation from three-phase current using Park's Transformation.

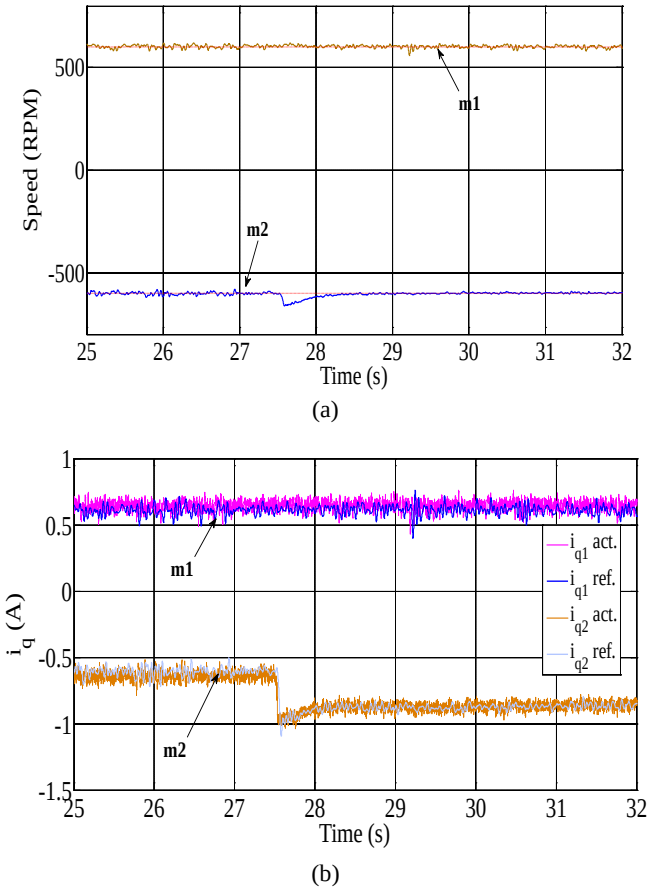

Figure 8.(a) - Speed responses for m1 and m2 for Dual-PMSM Drives during load condition, (b) – quadrature currents for m1 and m2.

Table 1. Specifications of M1 and M2

No	Motor Specifications	Value
1	Rated Torque	8Nm
2	Rated Speed	209rad/s
3	Inertia	0.0006329 kgm^2
4	Resistance	0.9585Ω
5	Inductance	0.00525H
6	Magnet Flux	0.1827Vs
7	DC Link Voltage	300V

4. CONCLUSION

The detailed performance investigation of speed behavior for Dual PMSM drives fed by FLI using sensorless technique is presented. An investigation is carried out for both PMSMs under different operating condition. The experimental results prove that the topology of a Five-Leg Inverter (FLI) is able to drive two different motors and for different operating conditions. Moreover, through the experimental works, the proposed controller which is Sensorless Drives for FLI also shows comparable results with the drives which using sensor.

ACKNOWLEDGEMENTS

The authors would like acknowledge Universiti Teknikal Melaka Malaysia and from the Ministry of Education of Malaysia for the financial support in order to carry out the research project.

REFERENCES

[1] S. N. Vukosavic, M. Jones, D. Dujic, and E. Levi, "An improved PWM method for a five-leg inverter supplying two three-phase motors," in *IEEE Symposium on Industrial Electronics 2008, ISIE 2008*, 2008, pp. 160-165.

[2] K. Oka, Y. Nozawa, and K. Matsuse, "Improved method of voltage utility factor for PWM control method of five-leg inverter," in *The 37th IEEE Conference on Power Electronics Specialists, 2006 (PESC'06)*, Jeju Island, Korea, 2006, pp. 1-5.

[3] M. Jones, S. Vukosavic, D. Dujic, E. Levi, and P. Wright, "Five-leg inverter PWM technique for reduced switch count two-motor constant power applications," *Electric Power Applications, IET*, vol. 2, pp. 275-287, 2008.

[4] C. B. Jacobina, E. C. dos Santos, E. R. C. da Silva, M. B. de Correa, A. M. N. Lima, and T. M. Oliveira, "Reduced Switch Count Multiple Three-Phase AC Machine Drive Systems," *Power Electronics, IEEE Transactions on*, vol. 23, pp. 966-976, 2008.

[5] P. Delarue, A. Bouscayrol, and B. Francois, "Control implementation of a five-leg voltage-source-inverter supplying two three-phase induction machines," in *IEEE International Conference on Electric Machines and Drives 2003, IEMDC'03*, 2003, pp. 1909-1915 vol. 3.

[6] B. Francois and A. Bouscayrol, "Design and modelling of a five-phase voltage-source inverter for two induction motors," 1999.

[7] B. Francois, P. Delarue, A. Bouscayrol, and J. Niiranen, "Five-leg ac-ac power converter: structure, modeling and control," 2000, pp. 1525-1532 vol. 3.

[8] A. Bouscayrol, B. Francois, P. Delarue, and J. Niiranen, "Control implementation of a five-leg AC-AC converter to supply a three-phase induction machine," *Power Electronics, IEEE Transactions on*, vol. 20, pp. 107-115, 2005.

[9] P. Delarue, A. Bouscayrol, and E. Semail, "Generic control method of multileg voltage-source-converters for fast practical implementation," *Power Electronics, IEEE Transactions on*, vol. 18, pp. 517-526, 2003.

[10] M. Jones, D. Dujic, and E. Levi, "A performance comparison of PWM techniques for five-leg VSIs supplying two-motor drives," in *34th Annual Conference of IEEE on Industrial Electronic 2008, IECON 2008*, 2008, pp. 508-513.

[11] M. Jones, S. N. Vukosavic, and E. Levi, "Parallel-Connected Multiphase Multidrive Systems With Single Inverter Supply," *Industrial Electronics, IEEE Transactions on*, vol. 56, pp. 2047-2057, 2009.

[12] E. Ledezma, B. McGrath, A. Munoz, and T. A. Lipo, "Dual AC-drive system with a reduced switch count," *Industry Applications, IEEE Transactions on*, vol. 37, pp. 1325-1333, 2001.

[13] Y. Kimura, M. Hizume, and K. Matsuse, "Independent vector control of two PM motors with five-leg inverter by the expanded two-arm modulation method," 2005, pp. 7 pp.-P. 7.

[14] Y. Ohama, K. Oka, and K. Matsuse, "Characteristic of independent two induction motor drives fed by a five-leg inverter," 2009, pp. 1-4.

[15] A. Rajasekhar, R. K. Jatoth, A. Abraham, and V. Snasel, "A novel hybrid ABF-PSO algorithm based tuning of optimal FOPI speed controller for PMSM drive," in *The 12th International Conference on Carpathian Control (ICCC2011)*, Velke Karlovice 2011, pp. 320-325.

[16] P. Pillay and R. Krishnan, "Modeling, simulation, and analysis of permanent-magnet motor drives. I. The permanent-magnet synchronous motor drive," *Industry Applications, IEEE Transactions on*, vol. 25, pp. 265-273, 1989.